Coincidence spectroscopy for increased sensitivity in radionuclide monitoring

P. Andersson[1], A. Göök[1], V. Rathore[1], E. Andersson Sundén[1], E. Branger[1], S. Grape[1], C. Gustavsson[1], V. Mishra[1], M. Preston[1], O. Khotiaintseva[1,2], V. Khotiaintsev[1,3], J. Kastlander[4], A. Ringbom[4]

[1] Uppsala University, Department of Applied Nuclear Physics

[2] Institute for Safety Problems of Nuclear Power Plants of NAS of Ukraine

[3] Taras Shevchenko National University of Kyiv

[4] Swedish Defence Research Agency (FOI)

Abstract

The majority of the energy in a nuclear explosion is released in the immediate blast and the initial radiation accounts. The remaining fraction is released through radioactive decay of the explosion's fission products and neutron activation products over a longer time span. This allows for the detection of a nuclear explosion by detecting the presence of residual decay. Radionuclide monitoring stations for detection of radioactive emissions to the atmosphere is thereby an important tool in the verification of compliance with nuclear disarmament treaties. In particular, the globally spanning radionuclide station network of the International Monitoring System (IMS) has been implemented for verification of the Comprehensive Nuclear-Test-Ban Treaty.

High Purity Germanium (HPGe) detectors are workhorses in radionuclide monitoring. The detection of characteristic gamma rays can be used to disclose the presence of signature nuclides produced in nuclear weapon tests. A particular development that has potential to improve the sensitivity of radionuclide monitoring is the coincidence technique where decaying nuclides that emit several coincident gamma rays can be detected at much smaller activity concentrations than with conventional gamma spectroscopy.

In this project, dedicated gamma-gamma coincidence detectors are being developed, utilizing electronically segmented HPGe detectors. These detectors are expected to be highly sensitive to low-activity samples of nuclides that present coincident emissions of gamma rays. In this paper we present the concept, define performance parameters, and explore the performance of such detectors to a subset of radionuclides of particular CTBT relevance. In addition, we discuss the path forward in developing a next generation gamma-gamma coincidence spectroscopy system of segmented HPGe.

1. Introduction

Many radionuclides are unique signatures to production or use of nuclear materials, and environmental monitoring is already performed for verification of the Comprehensive Test-Ban Treaty (CTBT). Although the treaty is not yet ratified, the International Monitoring System (IMS), which was set up for its verification, has more than 300 stations for remote sensors worldwide, 72 of which are certified radionuclide stations [1]. Also for other proposed treaties, such as the Fissile Material Cutoff Treaty (FMCT), radionuclide monitoring may in principle be useful, since fissile material production leads to releases of radionuclides from reactors and reprocessing facilities.

The origin of radionuclides is the fission process, which generates two fission products, and also the prompt emission of gamma and neutron radiation. The fission products are typically radioactive nuclides that will continue to decay for a long time after the fission chain reaction has ceased, and in this process they emit delayed fission gamma rays. Another source of radionuclides are the neutrons emitted by the fission reactions, which when captured by surrounding materials create activation products, some of which emit gamma rays. Because of delayed gamma radiation, any nuclear operations including fission chain reactions are in principle possible to detect by remote means, if the fission or activation products are to some extent dispersed in the environment. Monitoring such radionuclides in the atmosphere is an attractive means of technical verification, since the state of origin cannot refuse access to radionuclides that have already been dispersed by the winds from its territory.

There are two main categories of radionuclide detectors currently relied upon in the IMS, noble gas detectors and radioactive particle (aerosol) detector systems. Noble gas detectors include a gas collection system, typically for trapping xenon. The xenon is subsequently assessed for its radioactive inventory using the very sensitive coincidence technique, where the simultaneous detection of two radiation emissions from the same decaying nuclide is used to selectively examine the presence of the nuclides of interest in a background of other radiation [2], [3]. This way, very sensitive measurements of radioactive xenon can be made [3]. The multitude of radioactive xenon isotopes that can be assessed this way has also proved to be valuable in the discrimination of test explosions from background releases from civilian activities [4]. The effectiveness of radioxenon detectors was demonstrated in detection of actual nuclear tests by North Korea [5], [6].

Further adding to the capability of the International Monitoring System are radioactive particle detector systems [7], which form the majority of the IMS radionuclide stations. In such stations, radioactive aerosols are sampled using air filters and examined using gamma spectroscopy with High Purity Germanium (HPGe) detectors. This way, a large number of fission and activation products can be assessed; nearly a hundred radionuclides have been identified as relevant for the detection of nuclear tests [8]. The detection of these nuclides in air masses can provide evidence of nuclear operations, and help to deduce the cause and origin of such releases.

The nuclide identification in gamma spectroscopy is based on the detection of the characteristic gamma rays emitted by radionuclides. The precise energies of the gammas emitted are a fingerprint of the radionuclides, and the intensities are proportional to the amount of the respective nuclides. Detection of a nuclide is based on counting a number of characteristic gamma rays recorded in the detector, and if this is significantly above the background, the nuclide is detected. However, if the release of radioactivity from a treaty violation event is low, if the release is strongly diluted prior to being sampled, or if allowed to decay substantially, the activity reaching a monitoring station can be too low to result in a significant signal above the background. There is always background radiation present, e.g. from natural radiation sources, which may overlap with signals of interest, and hide a low-intensity signal in the noise. While ideally, non-detections of signature nuclides would mean that neither release nor a violation of a treaty took place, in practice they are associated with detection limits [9]. A rationale for lowering the detection limits is therefore that it widens the activity range for which detection is possible.

Coincidence detection is a way to lower the detection limits, making the monitoring more sensitive. Just as in radioxenon detection, this technique would be valuable also in gamma ray spectroscopy of any nuclides that emit multiple gammas. The coincidence technique is based on simultaneously detecting multiple gamma rays, using multiple detection elements. By only counting events where

two characteristic gamma rays are simultaneously registered, the probability of background to produce such matching events is very small, compared to matching only one energy. This leads to a dramatic reduction of background in coincidence measurements, and in turn to enhanced sensitivity.

In earlier works on coincidence detectors for radionuclide monitoring, the use of dual detector systems was already proposed, such as combining two planar HPGe detectors. This has indeed been demonstrated to lower the minimum detectable activity for some key nuclides [10], [11], [12]. However, we propose the further development toward multiple detection elements, and the evaluation of electronically segmented HPGe detectors for this purpose.

In this paper we present a tentative detector concept using segmented germanium. In addition, we present a simulation framework envisioned for use in the design and optimization of a finalized detector, and compare first simulation results with experimental data. Finally, we examine a list of key nuclides used for CTBT monitoring for correlated emissions of gamma rays, which is necessary for assay with coincidence spectroscopy.

2. Description of the proposed detector technique

Segmented HPGe detectors for coincidence spectroscopy offer two advantages compared to dual systems earlier proposed. Firstly, they can be of well type, as shown in figure 1, where the examined sample is inserted in the well. Thereby, the active volume covers nearly all directions from the sample. Secondly, a large number of elements can be used, up to 36 segments are commercially available. With such an increase of the number of detection elements that can score a coincidence event, substantial improvement can be anticipated. Segmented detectors of the type we propose use electronic segmentation, meaning that the active volume is a single solid germanium crystal, but it's effectively divided through segmentation of one of the contact electrodes that carries the electric signal.

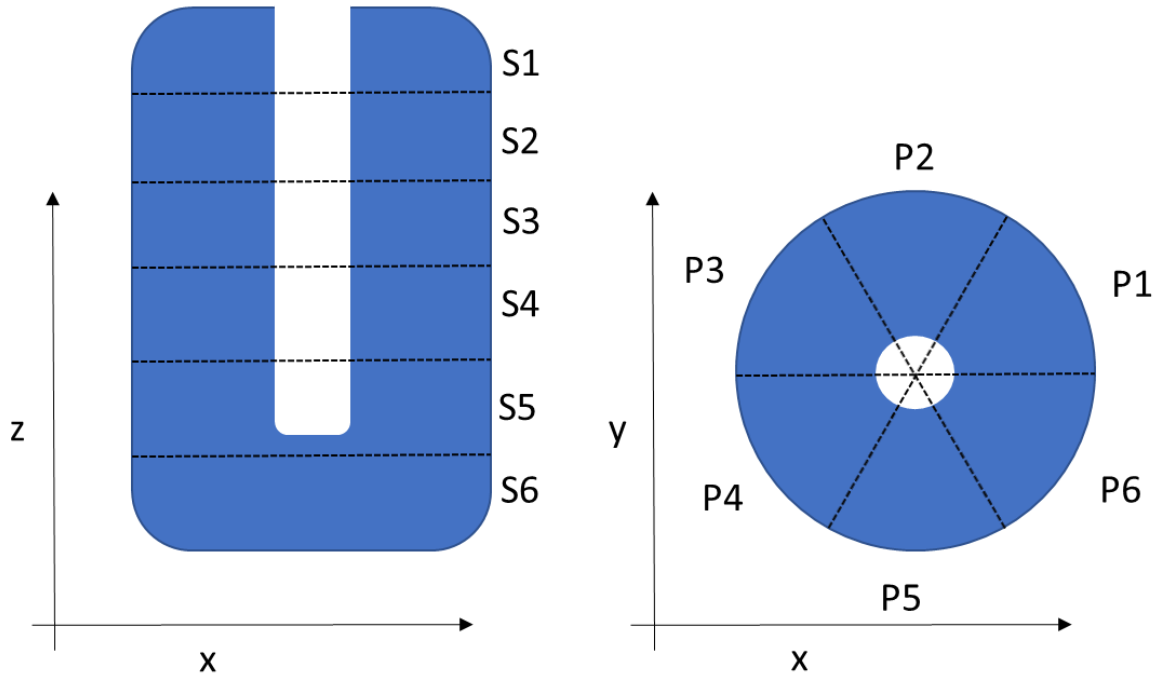

Figure 1. Conceptual illustration of a well-type coaxial HPGe detector crystal (blue) with a possible segmentation pattern (dashed black lines). There is extensive experience of manufacturing and use of up to 36 segments, 6

axial and 6 azimuthal, albeit the exact geometry and other parameters may differ in our final use. The sample under investigation is placed in the well.

The proposed technique gains benefits only if multiple gamma rays are emitted in a cascade upon the decay of a nuclide of interest. Lanthanum-140 is one example of a key nuclide of interest for CTBT that presents such a cascade of gamma rays that are for practical purposes simultaneous. Its decay scheme is presented in figure 2, includes many intensive gamma emissions following the beta decay, before reaching the stable ground state of the daughter, cerium-140. A table of other nuclides of interest for monitoring, and their suitability for coincidence spectroscopy, is presented in the Appendix.

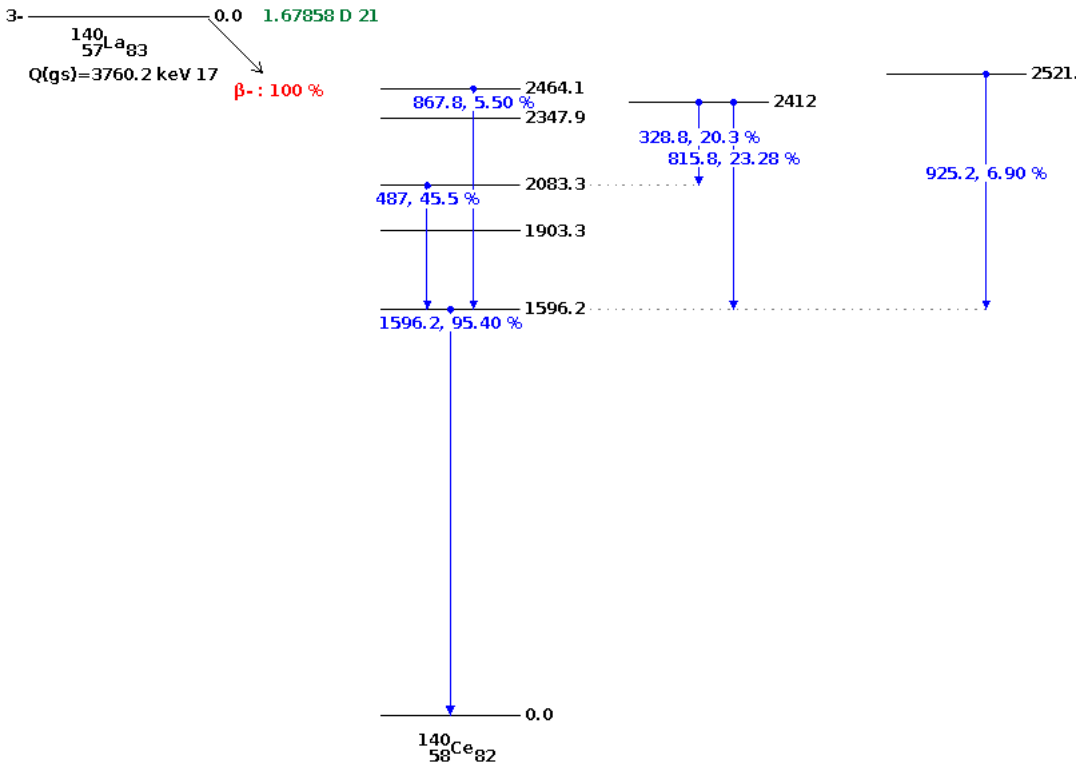

Figure 2. The decay scheme of La-140 (a key nuclide for CTBT monitoring), showing its six strongest-intensity gamma rays (blue). Following the transition from the precursor (lanthanum) to the daughter (cerium), many gamma transitions are possible. The most intensive gamma transition of 1596.2 keV is correlated with all the other five most intensive rays. La-140 can thus be noted as a promising candidate for coincidence spectroscopy, with multiple exploitable pairs of correlated gamma rays. (Nuclear data from the database NuDat 3.0.)

3. Simulation framework

Radiation simulation tools are essential in development of nuclear instruments such as radiation detectors. Clearly, a coincidence detector is not as simple to model as a conventional detector. In particular it requires a physics simulation code that includes both the full cascade decay, with time, direction and energy of all relevant correlated gamma emissions, and the subsequent gamma ray transport to and inside the detection elements.

A code framework that can perform this task is being assembled as a part of this project. The framework is built on the Monte-Carlo software Geant4 [18] [19] that simulates the decay of radionuclides, with the following chain of gamma emissions, on an event-by-event basis. In the

simulation, the emitted rays are also transported through the detector geometry, and the energy deposited in each sensing element is stored in a list, along with the time when the energy was deposited. This list can be further analyzed, analogously to how data from a real detector is treated.

4. First test of simulation framework

An experimental data collection was performed with an available segmented HPGe for the purpose of testing the simulation framework. The used detector has a cuboid active volume, with one large outer segment surrounding six small segments, as shown in figure 3. The small segments are very small and inefficient, due to their purpose in the original application of the used detector. Therefore, a so-called addback spectrum was created, where any coincident event in these six segments were summed, thereby creating a virtual segment corresponding to segments 1-6 in the figure below, while the larger outer segment was used as a separate element. Hence the detector operated in fact as a dual detector system.

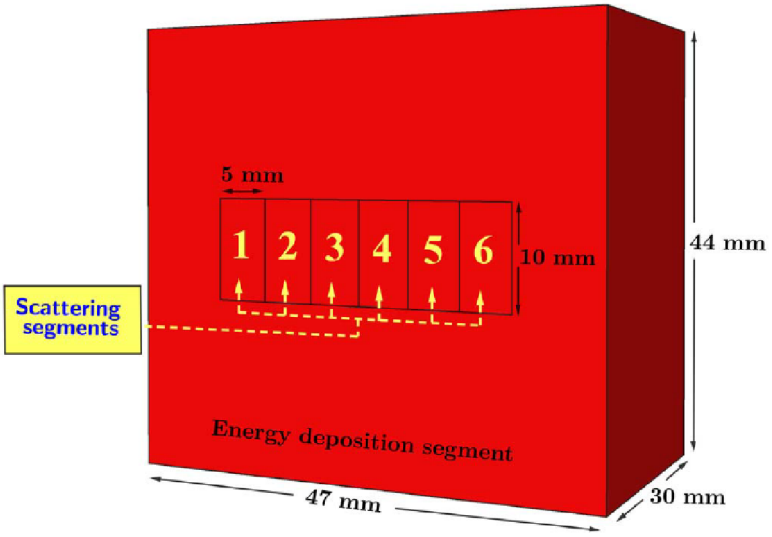

Figure 3. Active volume and segmentation of the test detector used for comparison between experiment and simulation. Image from [21]

It should be noted that this design differs from what would be used for a coincidence spectrometer, since the detector in question was designed and optimized for a different application, of gamma emission tomography [21], and not for the purpose as proposed in this work. However, the detector can still serve as demonstration of the nature of coincidence spectroscopy data, and for validation of the simulation framework.

Experimentally, we recorded a 2D pulse height spectrum of a Co-60 source, which has two coincident gamma rays at 1173 and 1332 keV; the spectrum is displayed in figure 4 below, compared with a simulation. The presented spectra show various features caused by coincident gamma rays, as well as caused by cross-talk of gammas scattering from one segment to another. The simulated and experimental spectra are qualitatively similar.

We plan to proceed to perform quantitative comparison between experimental and simulation data in order to validate the accuracy of the simulations, and after this proceed to using the simulation framework for optimization of a detector geometry for the purpose of coincidence spectroscopy. Establishing this simulation framework is an essential step in the successful design of a suitable and highly efficient detector.

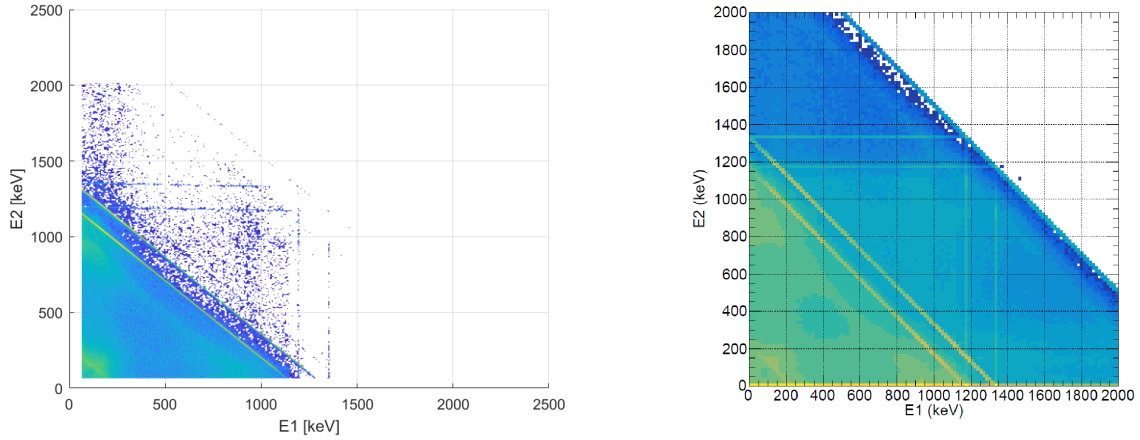

Figure 4. Left: Experimental 2D spectrum with segmented HPGe detector exposed to Co-60 sample emitting 1173 keV and 1332 keV gamma rays in coincidence. Right: Simulations results, showing similar features as the experimental data.

5. Evaluation of potential for assay of CTBT key nuclides

The main drawback of the gamma-gamma coincidence technique is that not all radionuclides emit multiple gamma rays in their decay. Therefore, the first priority in the examination of the usefulness of the technique is to investigate if there are nuclides of interest for monitoring in the nuclear disarmament regime, which are emitting a cascade of gamma.

For this purpose, we have performed a review of 87 radionuclides, which were previously identified as key nuclides for verification of the CTBT [8]. For each of these nuclides, the two most probable gamma and X-rays to be emitted in coincidence have been identified using the Geant4 code framework described in Section 4. Two gamma rays have to be emitted within a time span of 1 µs in order to be considered as a coincidence. In order not to include gamma rays with energies too low to be detectable an energy threshold of 30 keV is imposed. An upper limit of 10 days on the time span after the initial decay is also imposed, in order to remove the contribution of very long-lived progeny nuclides from the decay chain. All the investigated nuclides are listed in table 1 of the Appendix, with the most common coincident gamma-ray energies and the corresponding intensity per decay. Also listed in the table are energies and intensities of the gamma-ray transitions used in traditional single gamma-ray spectroscopy for comparison.

It was found that a substantial share of the nuclides has promising properties for their use in coincidence spectroscopy, where 31 nuclides have two gamma energies that are emitted in coincidence in more than 10% of the decays. These nuclides must be expected to be promising candidates for the proposed technique. In particular we want to highlight lanthanum-140, a strong gamma emitter that as aforementioned can be expected to more probably escape from an underground nuclear test due to being a progeny of xenon-140, a noble gas. However, the multitude of nuclides that offer coincident gamma emissions can also be valuable for discrimination of civilian background events. One example of the latter is cesium-134, which is produced in nuclear reactor

fuel, but not to a large extent in nuclear explosions, and is therefore useful to discriminate between different release types.

Conclusions

Gamma-gamma coincidence spectroscopy has been suggested over the recent decade for enhancing the sensitivity in radionuclide monitoring for CTBT verification. The current state of the art in this context is dual detector systems of HPGe. We propose the use of segmented HPGe detectors for the same purpose, which offers greater solid angle coverage as well as more sensing elements between which a coincidence event may take place.

It was found that due to the complexity of a coincidence detection system, modeling its performance will likely require a comprehensive simulation framework, which includes both the cascade decay of the nuclide as well as the gamma transport. A modeling framework using Geant4 is currently being prepared for such analysis, and the first comparison between simulated and experimental data has shown promising results, although quantitative analysis is not yet performed.

In an initial examination of a large number of key nuclides used in CTBT monitoring, it was found that a large share of such nuclides presents decays with correlated gamma emissions, and it is therefore concluded that the technique is promising. In particular, xenon progeny nuclides, such as lanthanum are considered promising nuclides to monitor in support of CTBT. It is suggested that further development and trial of this concept is undertaken, by completing the validation of the simulation framework, and applying it to the optimization of the detection efficiency of a key nuclide, such as La-140.

6. Acknowledgements

We would like to acknowledge the Alva Myrdal Centre for Nuclear Disarmament at Uppsala University for supporting this work.

[1] “CTBTO World Map.” https://www.ctbto.org/map/ (accessed Aug. 25, 2022).

[2] G. Le Petit *et al.*, “Spalax™ new generation: A sensitive and selective noble gas system for nuclear explosion monitoring,” *Applied Radiation and Isotopes*, vol. 103, pp. 102–114, Sep. 2015, doi: 10.1016/j.apradiso.2015.05.019.

[3] A. Ringbom, T. Larson, A. Axelsson, K. Elmgren, and C. Johansson, “SAUNA—a system for automatic sampling, processing, and analysis of radioactive xenon,” *Nuclear Instruments and Methods in Physics Research Section A: Accelerators, Spectrometers, Detectors and Associated Equipment*, vol. 508, no. 3, pp. 542–553, Aug. 2003, doi: 10.1016/S0168-9002(03)01657-7.

[4] M. B. Kalinowski and C. Pistner, “Isotopic signature of atmospheric xenon released from light water reactors,” *Journal of Environmental Radioactivity*, vol. 88, no. 3, pp. 215–235, Jan. 2006, doi: 10.1016/j.jenvrad.2006.02.003.

[5] A. Ringbom *et al.*, “Measurements of radioxenon in ground level air in South Korea following the claimed nuclear test in North Korea on October 9, 2006,” *Journal of radioanalytical and nuclear chemistry*, vol. 282, pp. 773–779, Dec. 2009, doi: 10.1007/s10967-009-0271-8.

[6] A. Ringbom *et al.*, “Radioxenon detections in the CTBT international monitoring system likely related to the announced nuclear test in North Korea on February 12, 2013,” *Journal of Environmental Radioactivity*, vol. 128, pp. 47–63, Feb. 2014, doi: 10.1016/j.jenvrad.2013.10.027.

[7] R. Werzi, “The operational status of the IMS radionuclide particulate network,” *J Radioanal Nucl Chem*, vol. 282, no. 3, p. 749, Jul. 2009, doi: 10.1007/s10967-009-0270-9.

[8] K. M. Matthews and L.-E. De Geer, “Processing of data from a global atmospheric radioactivity monitoring network for CTBT verification purposes,” *J Radioanal Nucl Chem*, vol. 263, no. 1, pp. 235–240, Jan. 2005, doi: 10.1007/s10967-005-0042-0.

[9] L. A. Currie, “Limits for qualitative detection and quantitative determination. Application to radiochemistry,” *Anal. Chem.*, vol. 40, no. 3, pp. 586–593, Mar. 1968, doi: 10.1021/ac60259a007.

[10] R. Britton, A. V. Davies, J. L. Burnett, and M. J. Jackson, “A high-efficiency HPGe coincidence system for environmental analysis,” *Journal of Environmental Radioactivity*, vol. 146, pp. 1–5, Aug. 2015, doi: 10.1016/j.jenvrad.2015.03.033.

[11] R. Britton and A. V. Davies, “Limits of detection — Enhancing identification of anthropogenic radionuclides,” *Nuclear Instruments and Methods in Physics Research Section A: Accelerators, Spectrometers, Detectors and Associated Equipment*, vol. 947, p. 162818, Dec. 2019, doi: 10.1016/j.nima.2019.162818.

[12] N. Marković, “Coincidence methods in gamma-ray spectrometry for radioecological applications,” p. 111.

[13] B. De Canditiis *et al.*, “Full-volume characterization of an AGATA segmented HPGe gamma-ray detector using a $$^{152}Eu$$source,” *Eur. Phys. J. A*, vol. 57, no. 7, p. 223, Jul. 2021, doi: 10.1140/epja/s10050-021-00537-1.

[14] B. Bruyneel *et al.*, “Crosstalk properties of 36-fold segmented symmetric hexagonal HPGe detectors,” *Nuclear Instruments and Methods in Physics Research Section A: Accelerators, Spectrometers, Detectors and Associated Equipment*, vol. 599, no. 2, pp. 196–208, Feb. 2009, doi: 10.1016/j.nima.2008.11.011.

[15] A. Pullia, D. Weisshaar, F. Zocca, and D. Bazzacco, “Cross-Talk Limits of Highly Segmented Semiconductor Detectors,” *IEEE Transactions on Nuclear Science*, vol. 58, no. 3, pp. 1201–1205, Jun. 2011, doi: 10.1109/TNS.2011.2129530.

[16] B. Bruyneel *et al.*, “Crosstalk corrections for improved energy resolution with highly segmented HPGe-detectors,” *Nuclear Instruments and Methods in Physics Research Section A: Accelerators, Spectrometers, Detectors and Associated Equipment*, vol. 608, no. 1, pp. 99–106, Sep. 2009, doi: 10.1016/j.nima.2009.06.037.

[17] R. Britton, M. J. Jackson, and A. V. Davies, “Quantifying radionuclide signatures from a γ–γ coincidence system,” *Journal of Environmental Radioactivity*, vol. 149, pp. 158–163, Nov. 2015, doi: 10.1016/j.jenvrad.2015.07.025.

[18] J. Allison *et al.*, “Recent developments in Geant4,” *Nuclear Instruments and Methods in Physics Research Section A: Accelerators, Spectrometers, Detectors and Associated Equipment*, vol. 835, pp. 186–225, Nov. 2016, doi: 10.1016/j.nima.2016.06.125.

[19] S. Hauf *et al.*, “Radioactive Decays in Geant4,” *IEEE Transactions on Nuclear Science*, vol. 60, no. 4, pp. 2966–2983, Aug. 2013, doi: 10.1109/TNS.2013.2270894.

[20] J. K. Tuli, “Evaluated nuclear structure data file,” *Nuclear Instruments and Methods in Physics Research Section A: Accelerators, Spectrometers, Detectors and Associated Equipment*, vol. 369, no. 2, pp. 506–510, Feb. 1996, doi: 10.1016/S0168-9002(96)80040-4.

[21] V. Rathore, L. Senis, P. Jansson, E. A. Sundén, A. Håkansson, and P. Andersson, “Calculation of Spatial Response of a Collimated Segmented HPGe detector for Gamma Emission Tomography by MCNP Simulations,” *IEEE Transactions on Nuclear Science*, pp. 1–1, 2022, doi: 10.1109/TNS.2022.3152056.

Appendix

Table 1. Key nuclides and gamma energies for CTBT verification. The gamma-gamma coincidence intensity is calculated by a Monte Carlo simulation generating repeated cascade decays with 10 000 samples. Therefore, an uncertainty in the order of a percent is anticipated. The single gamma intensities are retrieved from reference [8]. In particular the gamma-gamma coincidence intensity is important for the proposed application, and the higher the intensity, the better the potential to improve the sensitivity.

			gamma-gamma coincidence			single gamma	
Nuclide	Half-life		Energy1 (keV)	Energy2 (keV)	Intensity (%)	Energy (keV)	Intensity (%)
Antimony-120	5.76	d	704	1171	0.2	1171.7	100
Antimony-122	2.7238	d	693	564	3.7	564.2	69.3
Antimony-124	60.2	d	1691	603	46.6	602.7	97.8
Antimony-125	2.7582	y	428	31	3.1	427.9	29.6
Antimony-126	12.46	d	695	666	99.0	695	99.6
Antimony-127	3.85	d	604	473	3.6	685.7	36.8
Antimony-128	9.01	h	754	743	99.4	743.2	100
Arsenic-74	17.77	d	608	596	0.5	595.8	59.4
Arsenic-76	1.0778	d	657	559	5.9	559.1	45
Barium-133	10.52	y	31	356	29.8	356	62.05
Barium-140	12.752	d	487	1596	44.0	537.3	24.39
Cadmium-115	53.46	h	231	261	0.8	336.2	45.9
Cadmium-115m	44.6	d	484	934	0.3	933.8	2
Cerium-141	32.501	d	NA	NA	0.0	145.4	48.2
Cerium-143	33.039	h	293	36	23.1	293.3	42.8
Cerium-144	284.893	d	1489	697	0.2	133.5	11.09
Cesium-132	6.479	d	34	668	12.7	667.7	97.5
Cesium-134	2.0648	y	796	605	85.3	604.7	97.6
Cesium-136	13.16	d	1048	818	79.4	1048.1	80
Cesium-137	30.07	y	NA	NA	0.0	661.7	85.1
Chromium-51	27.702	d	NA	NA	0.0	320.1	10
Cobalt-57	271.79	d	570	122	0.0	122.1	85.6
Cobalt-58	70.82	d	864	811	0.7	810.8	99
Cobalt-60	1925.1	d	1173	1332	99.8	1332.5	100
Europium-152	13.537	y	40	122	17.4	1408	20.9
Europium-152m	9.3116	h	40	842	8.7	841.6	14.6
Europium-155	4.7611	y	45	43	0.4	105.3	21.2
Europium-156	15.19	d	646	1231	6.8	1153.7	6.8
Europium-157	15.18	h	411	43	3.7	370.5	11
Gallium-72	14.1	h	2202	834	26.7	834.1	95.6
Gold-196	6.183	d	67	356	33.8	355.7	86.9
Gold-196m	9.7	h	356	67	22.6	147.8	42.5
Gold-198	2.69517	d	676	412	0.7	411.8	96
Iodine-130	12.36	h	669	536	95.7	536.1	99
Iodine-131	8.0207	d	284	80	2.7	364.5	81.7
Iodine-133	20.8	h	856	530	1.5	529.9	87
Iodine-135	6.57	h	547	1132	6.9	1260.4	28.9
Iridium-190	11.78	d	605	558	23.8	186.7	52.4

Iridium-192	73.827	d	468	317	44.1	316.5	82.81
Iron-59	44.503	d	192	1099	3.3	1099.2	56.5
Lanthanum-140	1.6781	d	487	1596	45.5	1596.2	95.4
Lead-203	51.873	h	73	279	30.0	279.2	81
Manganese-54	312.12	d	NA	NA	0.0	834.8	100
Molybdenum-99	65.94	h	739	181	6.5	140.5	89.4
Neodymium-147	10.98	d	275	319	0.8	531	13.1
Neptunium-239	2.3565	d	106	104	7.9	277.6	14.38
Palladium-112	21.03	h	1388	618	5.3	617.5	43
Potassium-42	12.36	h	313	1525	0.3	1524.7	18.1
Promethium-149	53.08	h	305	286	0.0	286	3.1
Promethium-151	28.4	h	275	40	3.2	340.1	22.5
Radium-224	3.66	d	583	2615	29.9	241	4.1
Rhodium-102	207	d	628	475	4.9	475.1	47
Rhodium-105	35.36	h	39	281	0.0	319.1	19.2
Rubidium-84	32.77	d	1016	882	0.3	881.6	69
Ruthenium-103	39.26	d	557	53	0.3	497.1	90.9
Ruthenium-106	373.59	d	622	512	10.6	621.9	9.93
Samarium-153	46.27	h	42	103	3.9	103.2	31.4
Samarium-156	9.4	h	204	87	13.2	203.8	20.8
Scandium-46	83.79	d	1121	889	100.0	889.3	100
Silver-106m	8.28	d	717	512	29.4	717.2	28.9
Silver-108m	418	y	723	614	90.5	722.9	90.8
Silver-110m	249.79	d	885	658	72.8	658	94.0
Silver-111	7.45	d	97	245	0.1	342.1	6.7
Sodium-24	14.959	h	2754	1369	99.9	1368.6	100
Strontium-91	9.63	h	652	653	3.4	1024.3	33.4
Technetium-99m	6.01	h	NA	NA	0.0	140.5	89.1
Tellurium-129m	33.6	d	209	278	0.1	695.9	3.19
Tellurium-131m	30	h	794	852	13.2	773.7	49.9
Tellurium-132	3.204	d	773	668	75.3	772.6	75.6
Thulium-168	93.1	d	198	816	42.8	816	50
Tin-125	9.64	d	823	1067	4.1	1067.1	10
Tungsten-187	23.72	h	480	61	5.4	685.7	27.3
Uranium-237	6.75	d	102	60	8.3	208	21.2
Xenon-131m	11.84	d	NA	NA	0.0	163.9	1.91
Xenon-133	5.243	d	31	81	0.2	81	38
Xenon-133m	2.19	d	31	31	0.2	233.2	10
Xenon-135	9.14	h	158	250	0.4	249.8	90.2
Yttrium-88	106.65	d	898	1836	93.9	1836.1	99.2
Yttrium-93	10.18	h	1918	267	1.4	266.9	7.32
Zinc-65	244.26	d	NA	NA	0.0	1115.5	50.6
Zinc-69m	13.76	h	NA	NA	0.0	438.6	94.8
Zirconium-89	78.41	h	NA	NA	0.0	909	99.9
Zirconium-95	64.02	d	NA	NA	0.0	756.7	54.5
Zirconium-97	16.91	h	602	1148	1.5	743.4	93.1